

also wish to thank to T. Watanabe for his valuable suggestions on PLL circuits. Finally, they would like to thank Dr. T. Yamada for his helpful suggestions and encouragement.

REFERENCES

- [1] Y. Murakami and S. Itoh, "A bandpass filter using YIG film grown by LPE," in *IEEE-MTT-S Int. Microwave Symp. Dig.*, 1985, pp. 285-288.
- [2] Y. Murakami, T. Ohgihara, and T. Okamoto, "A 0.5-4.0 GHz tunable bandpass filter using YIG film grown by LPE," in *IEEE-MTT-S Int. Microwave Symp. Dig.*, 1987, pp. 371-372.
- [3] T. Ohgihara, Y. Murakami, and T. Okamoto, "A 0.5-2.0 GHz tunable bandpass filter using YIG film grown by LPE," *IEEE Trans. Magn.*, vol. MAG-23, no. 5, pp. 3745-3747, 1987.
- [4] N. K. Osbrink, "Earth-terminal design benefits from MMIC technology," *Microwave Syst. News*, vol. 16, Aug. 1986.
- [5] J. C. Papp and Y. Y. Koyano, "An 8-18-GHz YIG-tuned FET oscillator," *IEEE Trans. Microwave Theory Tech.*, vol. MTT-28, pp. 762-767, July 1980.
- [6] B. Lax and K. J. Button, *Microwave Ferrites and Ferrimagnetics*. New York: McGraw Hill, 1962.
- [7] Y. Mizunuma, T. Ohgihara, H. Nakano, T. Okamoto, and Y. Murakami, "A 13-GHz YIG-film tuned oscillator for VSAT applications," in *IEEE MTT-S Int. Microwave Symp. Dig.*, 1988, pp. 1085-1088.
- [8] F. M. Gardner, *Phaselock Techniques*. New York: Wiley, 1979.

Full-Wave Analysis of Coupled Finline Discontinuities

GIOVANNI SCHIAVON, PIERO TOGNOLATTI, MEMBER, IEEE,
AND ROBERTO SORRENTINO, SENIOR MEMBER, IEEE

Abstract — The general discontinuity problem of coupled finline sections is considered. Coupling may occur either along the sides of the slots (parallel coupled finlines) or through their ends (end-coupled finlines). A particular case is the inductive strip discontinuity already addressed in the literature. The analysis is carried out expanding the fields in terms of TE and TM modes in the transverse direction, according to the generalized transverse resonance method. End effects in coupled finline sections are pointed out. Computed results are in good agreement with both data from the literature and first experiments.

I. INTRODUCTION

Finline discontinuities are still the objective of several investigations since not many data are available to the circuit designer. Accurate characterizations are of fundamental importance in establishing a reliable basis for the design of finline circuits.

An important class of discontinuity problems is that of coupled finline sections. They are used in a number of components, such as bandpass and bandstop filters and couplers. Both parallel coupling and end coupling may be realized. Such configurations are depicted in Fig. 1(a) and (b). Fig. 1(c) shows the geometry of the unilateral coupled finline structure. For analysis purposes, as discussed below, the structure is enclosed by two conducting planes perpendicular to the axial z direction.

In Fig. 1(a) two finline sections shorted at one end are coupled along the length s . In the discontinuity structure of Fig. 1(b) the two offset finline sections are shifted apart by a separation s so that the coupling occurs essentially through the line ends. The configuration of Fig. 1(b) can be considered as a special case of Fig. 1(a) by allowing the coupled length s to assume negative values. Negative s values thus correspond to a separation $|s|$ between the shorted ends of the finlines.

Manuscript received April 14, 1988; revised August 22, 1988.
The authors are with the Dipartimento di Ingegneria Elettronica, Università Tor Vergata, Via Orazio Raimondo, I-00173 Roma, Italy.
IEEE Log Number 8824201.

Depending on the geometrical parameters, Fig. 1 can represent a number of different configurations. The uniform coupled line structure is recovered by letting $l_1 = l_2 = s > 0$. The inductive strip is a special case of Fig. 1(b) for zero line offset. Such a discontinuity problem has been studied by Koster and Jansen [1] and by Knorr and Deal [2] using the spectral-domain method.

The coupled finline discontinuity of Fig. 1 as well as the uniform coupled finline structure is analyzed in this paper using the generalized transverse resonance technique introduced in [3]. This method is well known, so it is only briefly reviewed in the next section. Results have been computed for both end-coupled and parallel coupled finlines and are presented in Section III. Good agreement has been found with the data available in [1] and [2] relative to the inductive strip.

II. METHOD OF ANALYSIS

The method is based on the computation of the resonant conditions of a finline cavity containing the discontinuity. The resonator is formed by placing electric (or magnetic) walls some distance apart from the discontinuity. Although higher order modes could be included in the analysis method, it is assumed that only the dominant mode can propagate in each finline section. Higher order modes excited at the discontinuity are assumed to have negligible amplitudes at the shorting planes. This condition can be met by shifting the terminal planes half a wavelength apart or by using magnetic walls a quarter of a wavelength apart. The discontinuity can then be modeled as a two-port network. Assuming losses to be negligible the two-port structure is characterized by three real parameters. For a given frequency, they are computed via the resonant lengths of the cavity, i.e., the distances l_1 and l_2 . These are obtained by a field analysis of the finline cavity, as described below.

This method is equivalent to the tangent method [4] for measuring the equivalent circuit parameters of a discontinuity. It is observed that no characteristic impedance definition is needed since only normalized impedances enter the resonant condition. The computed impedances of the equivalent two-port are automatically normalized with respect to the characteristic impedances of the two finlines.

Simplification of the problem is obtained when the structure is symmetrical, thus $Z_{11} = Z_{22}$ (i.e., $w_1 = w_2$, $f_1 = f_2$ or $f_1 = b - f_2 - w_2$, Fig. 1). Two real quantities are sufficient to fully characterize the symmetrical discontinuity. Let the terminal planes be placed symmetrically ($l_1 = l_2$). Two types of resonance occur depending on whether the voltages at the ports are equal or opposite. The even (e) and odd (o) resonance conditions are

$$\begin{aligned} Z_e + Z_{11} - Z_{12} &= 0 \\ Z_o + Z_{11} + Z_{12} &= 0 \end{aligned} \quad (1)$$

where

$$Z_{e,o} = j \tan(\beta l_{e,o}) \quad (2)$$

are the normalized impedances seen from the discontinuity in the even or odd resonance condition, $\beta = \beta_1 = \beta_2$ is the phase constant of both finlines, and l_e and l_o are the even and odd resonant lengths, respectively. From (1) one obtains the impedance parameters of the discontinuity as

$$Z_{11} = -(Z_e + Z_o)/2 \quad Z_{12} = -(Z_e - Z_o)/2. \quad (3)$$

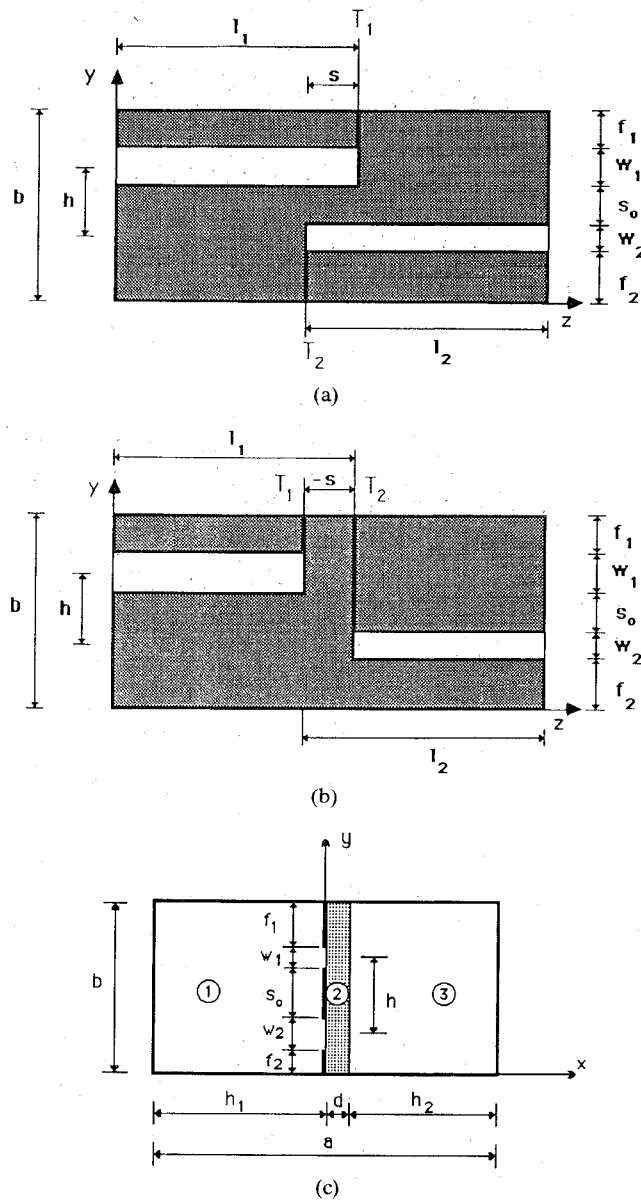


Fig. 1. (a) Longitudinal section of the parallel coupled finline discontinuity. (b) Longitudinal section of the offset end coupled finline discontinuity. (c) Cross-sectional geometry of the unilateral finline structure.

The discontinuity can be represented by a symmetrical T network, with series and shunt reactances $X_s = \text{Im}[Z_{11} - Z_{12}]$ and $X_c = \text{Im}[Z_{12}]$, respectively. These are expressed in terms of the even and odd resonant lengths as

$$\begin{aligned} X_s &= -\tan(\beta l_o) \\ X_c &= -[\tan(\beta l_e) - \tan(\beta l_o)]. \end{aligned} \quad (4)$$

The equivalent T network reduces to a simple shunt reactance when the odd resonant length is a multiple of half a wavelength ($X_s = 0$). The equality between the even and odd resonant lengths ($l_e = l_o$), on the contrary, corresponds to the two ports being decoupled ($X_c = 0$).

As indicated in Fig. 1, the equivalent network of the discontinuity is referred to the planes T_1, T_2 located at the finline ends. Such a choice is quite obvious for the end-coupled structure of Fig. 1(b), but might appear less natural for Fig. 1(a). However, it is preferable in the latter case too, since it leads to impedance

parameters with no polar singularities. For Fig. 1(a) another possibility would be that of interchanging the reference planes T_1 and T_2 , thus including the coupled line section between T_1 and T_2 . This choice of the reference planes leads, in the symmetrical case, to a new impedance matrix [Z'] having polar singularities when

$$(Z_{11} \pm Z_{21}) - j \cot \theta = 0 \quad (5)$$

where $\theta = \beta_s$. It is found that the above expression is equivalent to

$$l_{e,o} - s = (2n+1)\lambda/4 \quad (6)$$

n being an integer. When (6) is satisfied, an open circuit condition is produced at the new reference planes, in accordance with the impedance matrix [Z'] having a polar singularity. On the contrary, the impedance matrix [Z] at $T_1 T_2$ is generally well behaved.

Note that symmetry of the equivalent circuit ($Z_{11} = Z_{22}$) does not imply that in the structure of Fig. 1 there exists a symmetry plane which could be replaced by an electric or magnetic wall. For the parallel coupled finline discontinuity (Fig. 1(a)) symmetry can be of the polar type when $f_1 = f_2$ and $w_1 = w_2$. For the end-coupled discontinuity (Fig. 1(b)), symmetry can be of either the polar ($f_1 = f_2$) or the reflection type ($f_1 = b - f_2 - w_2$). Only in the last case does there exist a plane of symmetry so that the field analysis can be reduced to one half of the structure.

To determine the resonant lengths of the cavity, the electromagnetic (EM) field is expanded in terms of TE-to-x and TM-to-x modes in the dielectric and air regions (regions 1, 2, and 3 of Fig. 1(c)). In fact, looking in the transverse x direction, the structure is seen as a discontinuity problem in a rectangular waveguide of inner dimensions $l = l_1 + l_2 - s$ and b . On the plane of the fins, the electric field is zero everywhere except on the two slots, where it is expanded in terms of sets of orthogonal vector functions.

$$E_a^{(i)} = \sum_n V_n^{(i)} e_n^{(i)}, \quad i = 1, 2. \quad (7)$$

The e 's are chosen as the TE and TM eigenvectors of a waveguide with the same cross section as the slot pattern.

The boundary conditions on the fins' plane lead to a homogeneous system of equations in the field expansion coefficients in the various regions. By proper manipulation, the unknowns are reduced to only the expansion coefficients of the E field (7) in the slot regions. This greatly increases the numerical efficiency of the method in terms of both computer time and memory storage. In fact, only a few expansion terms are normally sufficient to represent the field on the slots, while a much higher number, typically b/w times higher, is required in the waveguide region to properly account for the edge condition [8]. An additional advantage is that no complex modes are involved. This is due to the EM field being expanded in homogeneous regions in terms of normal waveguide modes. On the contrary, the inclusion of complex modes in the modal spectrum of the finlines is required in the conventional mode-matching technique for an accurate evaluation of the characteristics of the discontinuity [9].

The condition for nontrivial solutions of the resulting homogeneous system constitutes the characteristic equation of the structure, as detailed in the Appendix. It is a function of frequency and line lengths l_1, l_2 . For any given frequency the characteristic equation is solved for three pairs of resonant lengths to compute through (1) the three unknown parameters of the discontinuity. Two pairs of (equal) lengths are computed for symmetrical

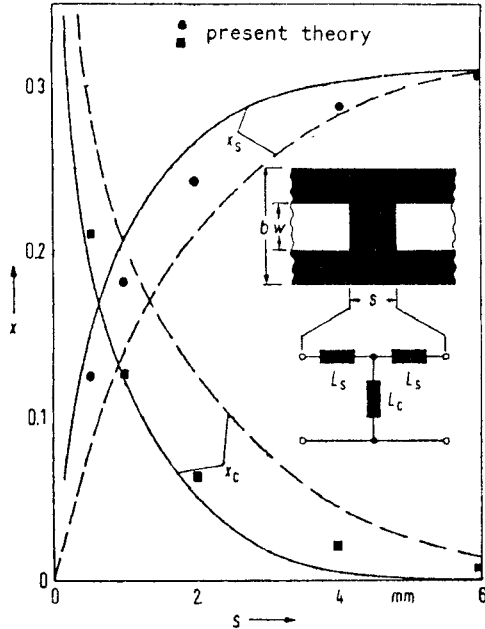


Fig. 2. Normalized reactances of the equivalent T network of a symmetrical inductive strip. WR28 waveguide; slot widths $w_1 = w_2 = 0.5$ mm. Substrate thickness $d = 0.254$ mm, $\epsilon_r = 2.22$, $f = 34$ GHz. Legend: — Koster and Jansen [1]; - - - Saad and Schuenemann [2].

structures. They correspond to the even (l_e) and odd (l_o) resonances.

As a particular case, when $l_1 = l_2 = s$ the method is used to compute the propagation characteristics of uniform coupled finlines. When no discontinuity is present the resonant condition is simply that the cavity length is a multiple of half a wavelength. The propagation constants at a given frequency are therefore evaluated from the resonant lengths of the cavity. Assuming the lowest order ($m = 1$) resonance, the propagation constant is simply $\beta = \pi/s$. Once the characteristic equation has been solved, the electromagnetic field distribution and all other related quantities, such as the characteristic impedance, can be computed [10].

III. RESULTS

The method has been tested by comparison with the results in [1] and [2]. The impedance parameters of the equivalent T network of a symmetrical inductive strip in unilateral finline are shown in Fig. 2 versus the longitudinal separation $|s|$. Both finlines are centered in the waveguide ($f_1 = b - f_2 - w_2$, $h = 0$). This figure has been taken from [1]. The computations of Saad and Schuenemann [5] are also reported. It is seen that the shunt reactance becomes negligible as the finline separation exceeds ≈ 6 mm, and the two finlines become practically uncoupled. The limit value of the series reactance X_s corresponds to the equivalent reactance of the end effect. Our computations are in good agreement with those of Koster and Jansen, although some shift toward Saad and Schuenemann's results is observed. Similar agreement with the results of [2] has been verified.

We next investigated the behavior of coupled finline lengths. Because of spurious effects at metal edges, the resonance lengths of the cavity containing the discontinuity are modified with respect to an ideal case. For comparison with the actual case, we have computed the resonant lengths of an ideal structure with no end effect, i.e., consisting of coupled lines terminated by ideal short circuits. The coupled lines have been characterized in terms of even and odd modes, the phase constant being computed by

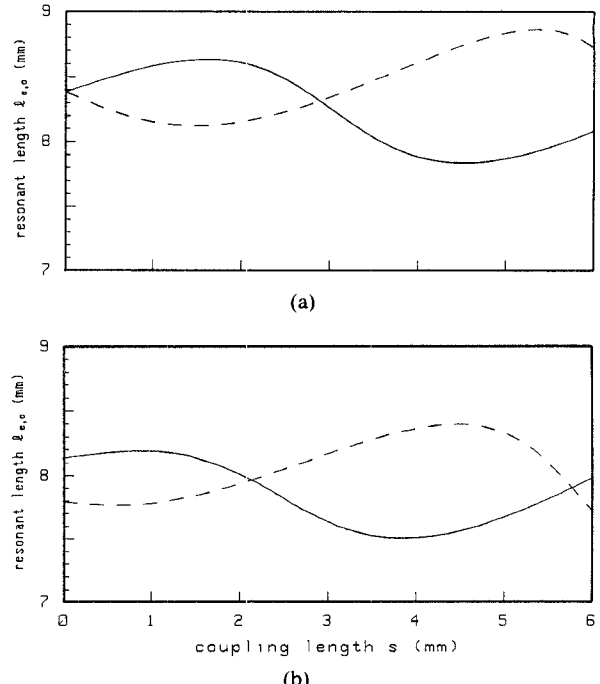


Fig. 3. Comparison of resonant lengths: (a) without end effect; (b) with end effect. WR28 waveguide; $f = 34$ GHz; slot widths $w_1 = w_2 = 0.5$ mm, $s_0 = 0.5$ mm, substrate thickness $d = 0.254$ mm, $\epsilon_r = 2.22$.

the transverse resonance method discussed at the end of the previous section. (Note that *even* and *odd* have a different meaning when referred to the resonant lengths l_e , l_o or to the coupled line modes.) The comparison is shown in Fig. 3(a) and (b) for a symmetrical structure at a frequency of 34 GHz. Only the case $s > 0$ is considered, since in the ideal case $s < 0$ is meaningless. For $s = 0$ no coupling occurs in the ideal case (Fig. 3(a)) so that $l_e = l_o$. In practice (Fig. 3(b)), owing to the end effect, the finline sections are still coupled even for $s = 0$, and different resonant lengths result in the even and odd cases. An oscillating behavior of the resonant lengths with the coupling length $s > 0$ is observed in both the ideal and real cases. It is observed that the end effect produces a shortening of the resonant lengths.

More extensive computations at different frequencies and for negative s values have shown [11] that the even and odd resonant lengths l_e and l_o tend to the same limit value as the separation/coupling length s becomes large and negative. This corresponds to the two finline sections being decoupled. Increasing s , l_e and l_o shift apart with an alternating behavior. For particular coupling lengths, which depend on the frequency, l_e and l_o become coincident again. Correspondingly, the shunt reactance X_c of the equivalent T network becomes zero. This can be observed in Fig. 4, where the normalized reactances of the equivalent T network referred to the planes T_1, T_2 of Fig. 1 are shown as a function of the separation/coupling s . (The absolute values of the reactances are obtained through multiplication by the characteristic impedances quoted in the caption. These have been computed using the voltage-power definition.) For large negative values of s the shunt reactance X_c is zero, while X_s tends to the limit value of the end effect for the isolated finline. The higher the frequency, the more pronounced the end effect, owing to the stronger excitation of higher order modes.

The influence of the transverse spacing s_0 (or, equivalently, of the line offset h) is shown in Fig. 5(a) and (b). The resonant

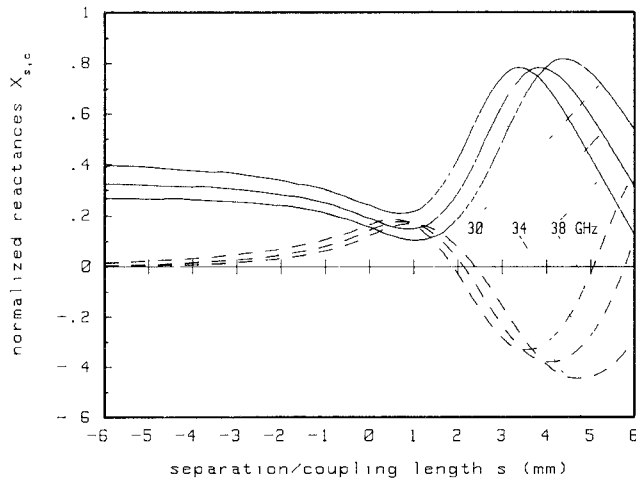


Fig. 4 Normalized reactances (— X_s ; --- X_c) of the equivalent T network of a symmetrical coupled finline discontinuity as a function of the separation/coupling length s . Reference planes are T_1 and T_2 of Fig. 1(a), (b). Finline characteristic impedances are $Z_0 = 209.3, 208.8, 210.0 \Omega$ at the frequencies of $f = 30, 34, 38$ GHz; slot widths $w_1 = w_2 = 0.5$ mm, $s_0 = 0.5$ mm, substrate thickness $d = 0.254$ mm, $\epsilon_r = 2.22$

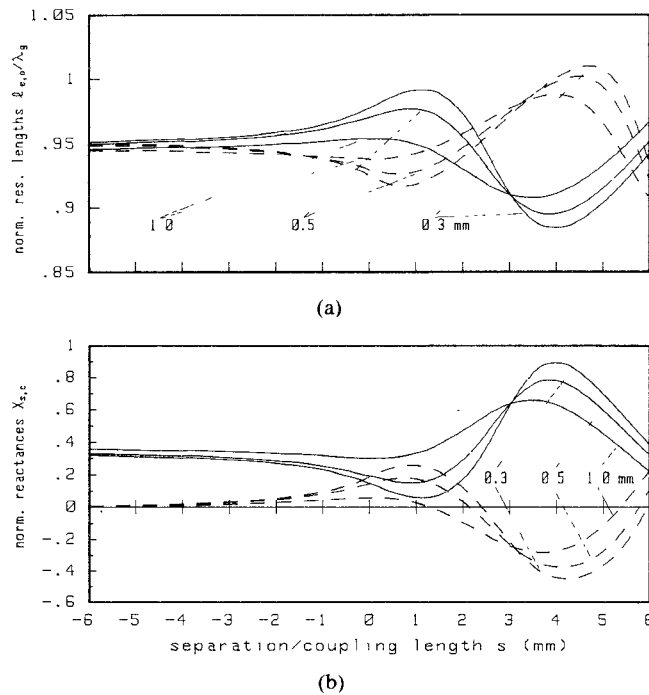


Fig. 5. Normalized resonant lengths (— l_s ; --- l_0) and T network normalized reactances (— X_s ; --- X_c) versus s , for different $s_0 = 1.0, 0.5, 0.3$ mm. Finline characteristic impedances are $Z_0 = 199.2, 208.8, 211.5 \Omega$, respectively. WR28 waveguide; slot widths $w = w_1 = w_2 = 0.5$ mm, substrate thickness $d = 0.254$ mm, $\epsilon_r = 2.22$, $f = 34$ GHz.

lengths and the T network reactances are plotted versus the longitudinal separation s for different transverse separation s_0 at $f = 34$ GHz. Lower values of s_0 produce stronger couplings, so that the resonant lengths depart more markedly from the limit value of $\approx 0.95\lambda_g$. A similar effect is observed on the reactance behavior. It can be noted that for a coupled length $s \approx 3$ mm the structure appears to be insensitive to variations of the transverse separation s_0 .

A discontinuity problem involving finlines with a narrower slot ($w = 0.3$ mm) is considered in Fig. 6(a) and (b). This case is

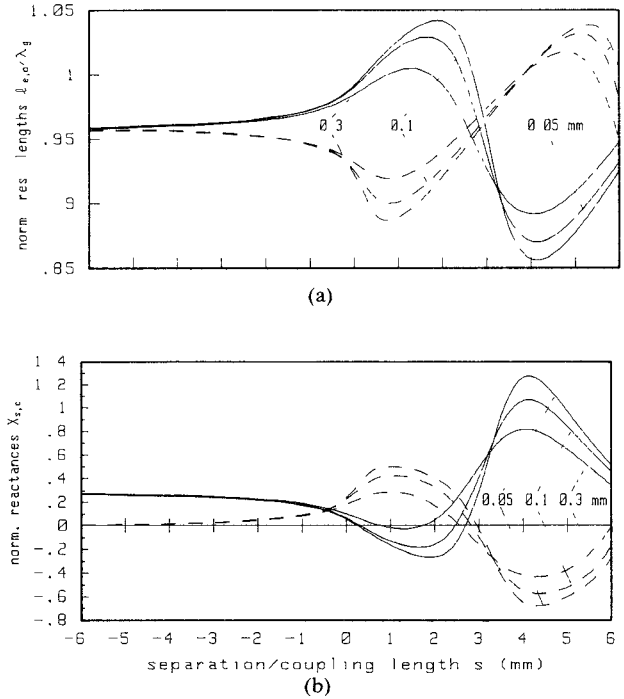


Fig. 6 Normalized resonant lengths (— l_s ; --- l_0) and T network normalized reactances (— X_s ; --- X_c) versus s , for different $s_0 = 0.3, 0.1, 0.05$ mm. Finline characteristic impedances are $Z_0 = 177.6, 178.3, 178.5 \Omega$, respectively. WR28 waveguide; slot widths $w = w_1 = w_2 = 0.3$ mm, substrate thickness $d = 0.254$ mm, $\epsilon_r = 2.22$, $f = 34$ GHz.

similar to that of Fig. 5, except more tightly coupled lines are considered. Because of the reduced transverse separation s_0 of the slots, the equivalent T network reactances undergo stronger variations. In particular, it is noted that the series reactance X_s exceeds unity for some ranges of the coupled length s for $s_0 = 0.1, 0.05$ mm. X_s assumes both positive and negative values depending on the coupled length s . For $s \ll 0$ (end effect of the isolated line) it is always inductive, while its reactive behavior may be reversed as s is made positive.

An experimental parallel coupled discontinuity structure was realized to verify the accuracy of the theory. Transitions to waveguide were realized as double exponential tapers (one wavelength long at 34 GHz). Two additional finline lengths (of length λ) were interposed between the tapers and the coupled section. The characteristics of the finline structure are quoted in the figure caption. A comparison of the theoretical and measured amplitudes of the scattering parameters is shown in Fig. 7. Measurements were made using an HP 8510 ANA. The agreement is considered fairly good. Discrepancies can be ascribed mainly to the behavior of the transitions and to the imperfect construction of the waveguide housing. The figure also shows the predicted behavior of the ideal coupled line structure with no end effect. It is observed that the present model represents a substantial improvement with respect to the idealized model.

IV. CONCLUSIONS

A general approach to the characterization of both uniform and discontinuous coupled finline structures has been presented. The analysis method is the generalized transverse resonance technique of [3]. Both parallel coupling and end coupling between offset lines have been considered. The analysis has been restricted to symmetrical configurations, ignoring the effect of the metallization thickness, but could be extended to these cases

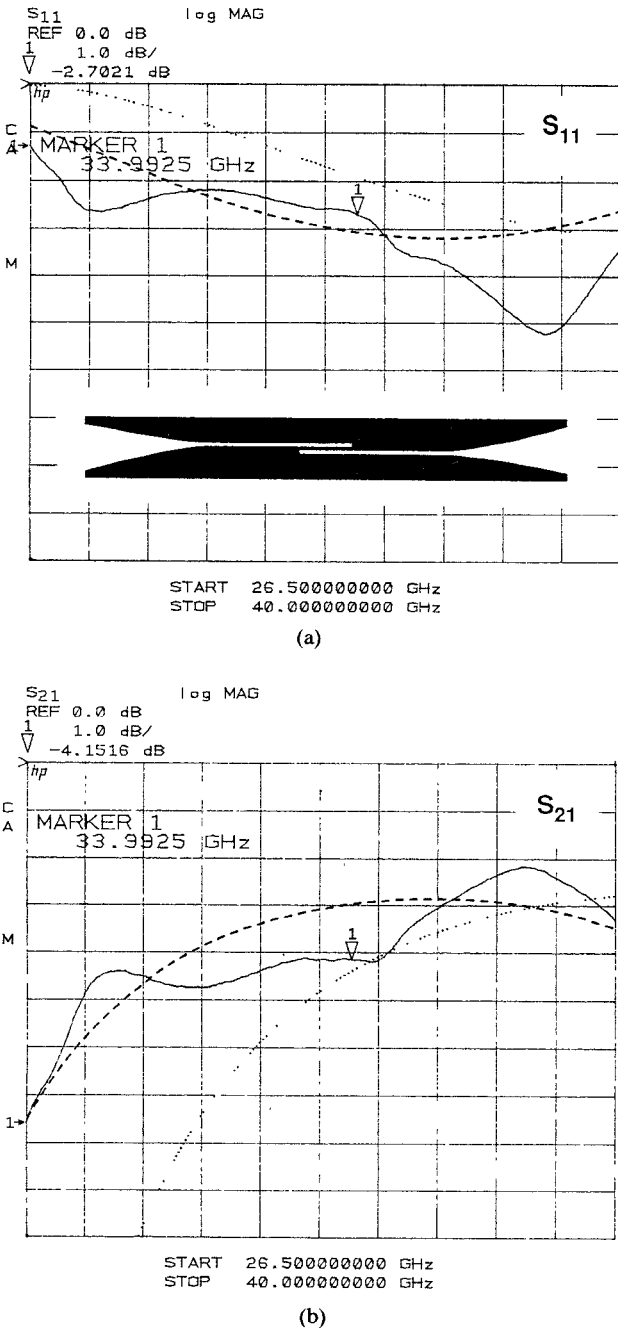


Fig. 7. Scattering parameters of a parallel coupled finline discontinuity
— Measurement; --- Present theory; ····· Simplified model. WR28
waveguide; $w_1 = w_2 = 0.356$ mm, $s = 4.0$ mm, $s_0 = 0.178$ mm, $d = 0.254$ mm,
 $\epsilon_r = 2.22$.

as well. The theory is confirmed by comparisons with data available in the literature and with first experiments.

APPENDIX

The homogeneous linear system of equations in the unknowns $V_n^{(i)}$ of the expansion (7) is obtained by imposing the continuity of the tangential magnetic field across the slots [10]. The condition for nontrivial solution determines the characteristic equation, i.e.,

$$\det \left[[T]^T ([Y_1] + [Y_2]) [T] \right] = 0. \quad (A1)$$

The $[T]$ matrix operates the transformation from the space of the basis functions used for the E -field expansion on the slots to that

of the basis functions ($TE^{(x)}$ and $TM^{(x)}$ modes) in the waveguide. The transposed matrix $[T]^T$ performs the inverse operation. Each column of $[T]$ corresponds to a basis function on the slots, while each row corresponds to a mode in the waveguide. Thus, the generic element $t_{\mu, \nu}$ of $[T]$, which relates the μ th term of waveguide field expansion with the ν th term of slot field expansion, falls into one of the following categories:

i) μ corresponds to a $TE_{pq}^{(x)}$ mode of the waveguide; ν corresponds to a $TE_{mn}^{(x)}$ mode of the i th slot:

$$t_{\mu, \nu} = \gamma_{m, n}^{(i)2} \iint_{S_{a_i}} \psi_{m, n}^{(i)} \psi_{p, q}^{(0)} dz dy. \quad (A2)$$

Here S_{a_i} is the i th slot, the ψ 's are the proper scalar potential functions (see below) and

$$\gamma_{m, n}^{(i)2} = \left(\frac{m\pi}{l_i} \right)^2 + \left(\frac{n\pi}{w_i} \right)^2. \quad (A3)$$

ii) μ corresponds to a $TE_{pq}^{(x)}$ mode of the waveguide; ν corresponds to a $TM_{mn}^{(x)}$ mode of the i th slot:

$$t_{\mu, \nu} = \oint_{\partial S_{a_i}} \psi_{m, n}^{(i)} \frac{\partial \varphi_{p, q}^{(0)}}{\partial \tau} d\gamma. \quad (A4)$$

Here ∂S_{a_i} is the boundary of the i th slot, $\partial/\partial\tau$ is the derivative along the tangent to ∂S_{a_i} , the φ 's are the proper scalar potential functions (see below), and $d\gamma$ is the length element.

iii) μ corresponds to a $TM_{pq}^{(x)}$ mode of the waveguide; ν corresponds to a $TE_{mn}^{(x)}$ mode of the i th slot:

$$t_{\mu, \nu} = 0. \quad (A5)$$

iv) μ corresponds to a $TM_{pq}^{(x)}$ mode of the waveguide; ν corresponds to a $TM_{mn}^{(x)}$ mode of the i th slot:

$$t_{\mu, \nu} = \gamma_{p, q}^{(0)2} \iint_{S_{a_i}} \varphi_{m, n}^{(i)} \varphi_{p, q}^{(0)} dz dy \quad (A6)$$

where

$$\gamma_{p, q}^{(0)2} = \left(\frac{p\pi}{l} \right)^2 + \left(\frac{q\pi}{b} \right)^2 \quad (A7)$$

with

$$l = l_1 + l_2 - s.$$

The form of the above expressions (A2), (A4), and (A6) has been obtained via application of Green's theorem.

The scalar potential functions ψ 's and φ 's in the waveguide have the following expressions:

$$\begin{aligned} \varphi_{p, q}^{(0)} &= P_{p, q}^{(0)} \sin \frac{p\pi z}{l} \sin \frac{q\pi y}{b} \\ \psi_{p, q}^{(0)} &= P_{p, q}^{(0)} \cos \frac{p\pi z}{l} \cos \frac{q\pi y}{b} \end{aligned} \quad (A8)$$

where

$$P_{p, q}^{(0)} = \sqrt{\frac{\delta_p \delta_q}{lb}} \frac{1}{\gamma_{p, q}^{(0)}} \quad (A9)$$

with

$$\delta_j = \begin{cases} 1 & \text{if } j = 0 \\ 2 & \text{if } j \neq 0 \end{cases}$$

Similar expressions hold for the ψ 's and φ 's on the i th slot.

$[Y_1]$ and $[Y_2]$ are diagonal matrices that relate the H field to the E field on the plane $x = 0$ in the rectangular waveguide. The

elements of these matrices are

$$y_{1_{\mu,\mu}} = -j\eta_{p,q} \cot(k_{p,q}h_1) \quad (A10)$$

$$y_{2_{\mu,\mu}} = J \frac{\eta'_{p,q} \tan(k'_{p,q}d) - \eta_{p,q} \cot(k_{p,q}h_2)}{1 + (\eta_{p,q}/\eta'_{p,q}) \tan(k'_{p,q}d) \cot(k_{p,q}h_2)} \quad (A11)$$

where

$$k_{p,q}^2 = \omega^2 \mu_0 \epsilon_0 - \gamma_{p,q}^{(0)^2} \quad k'_{p,q}^2 = \omega^2 \mu_0 \epsilon_0 \epsilon_r - \gamma_{p,q}^{(0)^2}. \quad (A12)$$

If μ correspond to a $TE_{p,q}^{(x)}$ mode of the waveguide,

$$\eta_{p,q} = \frac{k_{p,q}}{\omega \mu_0} \quad \eta'_{p,q} = \frac{k'_{p,q}}{\omega \mu_0} \quad (A13)$$

whereas if μ correspond to a $TM_{p,q}^{(x)}$ mode of the waveguide,

$$\eta_{p,q} = \frac{\omega \epsilon_0}{k_{p,q}} \quad \eta'_{p,q} = \frac{\omega \epsilon_0 \epsilon_r}{k'_{p,q}}. \quad (A14)$$

ACKNOWLEDGMENT

F. Melai of Micrel S.p.a., Florence, is gratefully acknowledged for performing the experimental work and the measurements.

REFERENCES

- [1] N. H. L. Koster and R. H. Jansen, "Some new results on the equivalent circuit parameters of the inductive strip discontinuity in unilateral fin lines," *Arch. Elek. Übertragung*, vol. 35, pp. 497-499, 1981.
- [2] J. B. Knorr and J. C. Deal, "Scattering coefficients of an inductive strip in a finline: Theory and experiment," *IEEE Trans. Microwave Theory Tech.*, vol. MTT-33, pp. 1011-1017, Oct. 1985.
- [3] R. Sorrentino and T. Itoh, "Transverse resonance analysis of finline discontinuities," *IEEE Trans. Microwave Theory Tech.*, vol. MTT-32, pp. 1633-1638, Dec. 1984.
- [4] R. E. Collin, *Field Theory of Guided Waves*. New York: McGraw-Hill, 1960, sec. 8.1.
- [5] A. M. K. Saad and K. Schuenemann, "A rectangular waveguide equivalent for bilateral and unilateral fin lines," *Arch. Elek. Übertragung*, vol. 35, pp. 287-292, 1981.
- [6] V. K. Tripathi, "Asymmetric coupled transmission lines in an inhomogeneous medium," *IEEE Trans. Microwave Theory Tech.*, vol. MTT-23, pp. 734-739, Sept. 1975.
- [7] R. H. Jansen, "Unified user-oriented computation of shielded, covered and open planar microwave and millimeter-wave transmission-line characteristics," *Microwave Opt. Acoust.*, vol. 3, pp. 14-22, Jan. 1979.
- [8] S. W. Lee, W. R. Jones, and J. J. Campbell, "Convergence of numerical solutions of iris-type discontinuity problems," *IEEE Trans. Microwave Theory Tech.*, vol. MTT-19, pp. 528-536, June 1971.
- [9] A. S. Omar and K. Schuenemann, "The effect of complex modes at finline discontinuities," *IEEE Trans. Microwave Theory Tech.*, vol. MTT-34, pp. 1508-1514, Dec. 1986.
- [10] G. Schiavon, R. Sorrentino, and P. Tognolatti, "Characterization of coupled finlines by generalized transverse resonance method," *Int. J. Numerical Modeling: Electronic Networks, Devices and Fields*, vol. 1, no. 1, pp. 45-59, Mar. 1988.
- [11] G. Schiavon, P. Tognolatti, and R. Sorrentino, "Fullwave analysis of coupled finline discontinuities," in *1988 Int. Microwave Symp. Dig.*, pp. 725-728.